*ФИЗИКА ЭЛЕМЕНТАРНЫХ ЧАСТИЦ И АТОМНОГО ЯДРА*
*2015. Т. 46. ВЫП. 5*

# HYPERON PUZZLE IN COMPACT STARS

*I. Bednarek* *

Institute of Physics, University of Silesia, Katowice, Poland

The objective of this paper is to solve the problem of the existence of hyperons in the interior of massive neutron stars. Using the more sophisticated equation of state with the extended sector of vector mesons, the model of a massive neutron star that includes hyperons was constructed.

PACS: 97.60.Jd; 26.60.-c

## INTRODUCTION

Realistic models of neutron stars take into account stratification of their internal structure. Very general description of neutron stars shows that they are composed of two main parts: a crust and a core. The crust, which splits into the outer and inner parts, describes the outer layer of a neutron star with subsaturation densities and contains only a small percentage of a neutron star mass [1]. Therefore, the total mass of a neutron star is almost entirely determined by the mass of its core. The density that characterizes the core of a neutron star ranges from a few times the saturation density ($n_0$) to about an order of a magnitude higher and at such densities hyperons are expected to emerge [2]. This paper has the goal of furthering the understanding of the existence of hyperons in neutron star interiors and is closely connected with the discovery of massive neutron stars. Observations of the binary millisecond pulsars J1614-2230 [3] and J0348 + 0432 [4] have led to the precise estimation of neutron star masses: $(1.97 \pm 0.04)M_{\odot}$ and $(2.01 \pm 0.04)M_{\odot}$. The existence of such massive neutron stars entails profound consequences for the equation of state (EoS) of dense nuclear matter by imposing constraints on the form of the EoS. High values of neutron star masses rule out most of the EoSs with hyperons because maximum masses achievable within models that involve exotic particles are well below the stated values. This in turn makes problematic the existence of hyperons in the very inner part of a neutron star.

*E-mail: ilona.bednarek@us.edu.pl

## 1. NEUTRON STAR MAXIMUM MASS

The value of the total mass and the radius of a neutron star can be calculated with the use of the Tolman–Oppenheimer–Volkoff (TOV) equation

$$\frac{d\mathcal{P}}{dr} = \frac{-G(\mathcal{E}(r) + \mathcal{P}(r))(m(r) + 4\pi r^3 \mathcal{P}(r))}{r^2 \left(1 - \dfrac{2Gm(r)}{r}\right)}, \tag{1}$$

$$\frac{dm}{dr} = 4\pi r^2 \mathcal{E}(r). \tag{2}$$

The above equations supplemented with the EoS ($\mathcal{P}(r) = \mathcal{P}(\mathcal{E}(r))$) allow one to calculate the mass–radius relation and additionally to model the internal structure of a neutron star, $\mathcal{E}$ denotes the energy density of a neutron star matter. This provides data on the impact of parameters of a given model on the internal structure of a neutron star.

## 2. FORMALISM

The theoretical description of strangeness-rich nuclear matter requires the inclusion of the full octet of baryons, additional hidden-strangeness meson fields $(\sigma^*, \varphi_\mu)$ should also be introduced to reproduce the hyperon–hyperon interaction. The EoS used to analyze the properties of a hyperon-rich neutron star was constructed within the framework of the nonlinear realization of the chiral $SU(3)_L \times SU(3)_R$ symmetry [5, 6]. As the model describes the $\beta$-equilibrated neutron star matter, the inclusion of leptons is necessary. Thus, the main components of the model are baryons $B = \{n, p, \Lambda, \Sigma^+, \Sigma^0, \Sigma^-, \Xi^0, \Xi^-\}$, mesons $M = \{\sigma, \omega_\mu, \rho^a_\mu\} \cup \{\sigma^*, \varphi_\mu\}$ and leptons $L = \{e^-, \mu^-\}$. The Lagrangian density of the model has the form

$$\begin{aligned}\mathcal{L} = \sum_B \overline{\psi}_B(i\gamma^\mu D_\mu - m_{\mathrm{eff},B})\psi_B + \frac{1}{2}\partial^\mu\sigma\partial_\mu\sigma + \frac{1}{2}\partial^\mu\sigma^*\partial_\mu\sigma^* - \frac{1}{2}m^2_{\sigma^*}\sigma^{*2} + \\ + \frac{1}{2}m^2_\omega(\omega^\mu\omega_\mu) + \frac{1}{2}m^2_\rho(\rho^{\mu a}\rho^a_\mu) + \frac{1}{2}m^2_\phi(\phi^\mu\phi_\mu) - \frac{1}{4}\Omega^{\mu\nu}\Omega_{\mu\nu} - \\ - \frac{1}{4}R^{\mu\nu}R_{\mu\nu} - \frac{1}{4}\Phi^{\mu\nu}\Phi_{\mu\nu} + U_{\mathrm{scalar}}(\sigma) + U^{\mathrm{vec}}_{\mathrm{nonl}}(\omega_\mu, \rho^a_\mu, \varphi_\mu) + \mathcal{L}_l,\end{aligned} \tag{3}$$

where the covariant derivative equals $D_\mu = \partial_\mu + ig_{B\omega}\omega_\mu + ig_{B\phi}\phi_\mu + ig_{B\rho}\mathbf{I}_B\boldsymbol{\rho}_\mu$, $\mathbf{I}_B$ denotes isospin of baryon $B$, $\Omega_{\mu\nu}$, $R^{\mu\nu}$ and $\Phi_{\mu\nu}$ are the field tensors of the $\omega$, $\rho$, and $\phi$ mesons fields. The Lagrangian density of free leptons is given by $\mathcal{L}_l = \sum\limits_{l=e,\mu} \overline{\psi}_l(i\gamma^\mu\partial_\mu - m_l)\psi_l$. The characteristic feature of the model is the very special form of the vector meson sector, which permits more accurate description of asymmetric strangeness-rich neutron star matter [7, 8]:

$$U_{\rm nonl}^{\rm vec}(\omega,\rho,\phi) = \frac{1}{4}c_3(\omega^\mu\omega_\mu)^2 + \frac{1}{4}c_3(\rho^{\mu a}\rho_\mu^a)^2 + \Lambda_V(g_{N\omega}g_{N\rho})^2(\omega^\mu\omega_\mu)(\rho^{\mu a}\rho_\mu^a) + \\ + \frac{1}{4}\left(\frac{1}{2}c_3 + \Lambda_V(g_{N\omega}g_{N\rho})^2\right)(\phi^\mu\phi_\mu)^2 + \\ + \frac{1}{2}\left(\frac{3}{2}c_3 - \Lambda_V(g_{N\omega}g_{N\rho})^2\right)(\omega^\mu\omega_\mu + \rho^{\mu a}\rho_\mu^a)(\phi^\mu\phi_\mu). \quad (4)$$

The primary goal of this paper is to maximize the understanding of the influence of the nonlinear vector meson couplings on the form of the EoS and through this on a neutron star mass and structure. The potential (4) includes coupling of different types between vector mesons. This allows one to modify the behaviour of the EoS in the high density limit. The Lagrangian function (3) makes it possible to calculate the equations of motion from the corresponding Euler–Lagrange equations. Analysis of the equations of motion raises the issue of the medium effects on the properties of the hadronic matter, namely, the effective baryon and vector meson masses that are given by the following relations:

$$m_{{\rm eff},B} = m_{{\rm eff},B}(s_0, s_0^*) = m_B - g_{B\sigma}s_0 - g_{B\sigma^*}s_0^*, \quad (5)$$

$$m_{{\rm eff},\omega}^2 = m_\omega^2 + 3c_3w_0^2 + 2\Lambda_V(g_{B\omega}g_{B\rho})^2r_0^2 + \left(\frac{3}{2}c_3 - \Lambda_V(g_{B\omega}g_{B\rho})^2\right)f_0^2,$$
$$m_{{\rm eff},\rho}^2 = m_\rho^2 + 3c_3r_0^2 + 2\Lambda_V(g_{B\omega}g_{B\rho})^2w_0^2 + \left(\frac{3}{2}c_3 - \Lambda_V(g_{B\omega}g_{B\rho})^2\right)f_0^2, \quad (6)$$
$$m_{{\rm eff},\varphi}^2 = m_\varphi^2 + \left(\frac{3}{2}c_3 - \Lambda_V(g_{B\omega}g_{B\rho})^2\right)(w_0^2 + r_0^2) + \left(\frac{3}{4}c_3 + \Lambda_V(g_{B\omega}g_{B\rho})^2\right)f_0^2.$$

The obtained results were calculated in the mean-field approximation and $s_0, s_0^*$, $w_0, r_0, f_0$ are the classical mean-field values of the meson fields. The description of dense, hyperon-rich nuclear matter given by the Lagrangian (3) in the case of nonstrange matter is reduced to the standard TM1 [9] model with an extended isovector sector. This extension refers to the presence of the $\omega-\rho$ meson coupling and enables modification of the high density limit of the symmetry energy. The strength of this coupling is characterized by the parameter $\Lambda_V$. For each value of the parameter $\Lambda_V$, the parameter $g_{N\rho}$ has to be adjusted to reproduce the symmetry energy $E_{\rm sym} = 25.68$ MeV at $k_F = 1.15$ fm$^{-1}$ [10]. The knowledge of the coupling constants that describe baryon interactions in the strange sector of the model is essential for the correct construction of the EoS. However, the incompleteness of the experimental data intensifies the uncertainties that are connected with the evaluation of coupling constants that involve strange baryons.

Hyperon–vector meson coupling constants are taken from the quark model. In the scalar sector, the scalar couplings $g_{B\sigma}$ of the $\Lambda$, $\Sigma$ and $\Xi$ hyperons require constraining in order to reproduce the estimated values of the potentials felt by a single $\Lambda$, $\Sigma$ and $\Xi$ in the saturated nuclear matter, the following values of the potentials were used:

$$U_{\Lambda}^{(N)} = -28\ \mathrm{MeV}, \quad U_{\Sigma}^{(N)} = +30\ \mathrm{MeV}, \quad U_{\Xi}^{(N)} = -18\ \mathrm{MeV}. \tag{7}$$

The coupling of hyperons to the strange meson $\sigma^*$ were obtained from the following relations [11]:

$$U_{\Xi}^{(\Xi)} \simeq U_{\Lambda}^{(\Xi)} \simeq 2U_{\Xi}^{(\Lambda)} \simeq 2U_{\Lambda}^{(\Lambda)}. \tag{8}$$

## 3. NUMERICAL RESULTS

Results of the numerical solutions that were obtained for TM1 parameterization are shown in Fig. 1. Calculations have been done for the nucleon matter and the strangeness-rich neutron star matter. This figure shows that the stiffness of the EoS depends on the existence and strength of the mixed vector meson interactions, and the extended nonlinear model makes it possible to construct a much stiffer EoS than the one obtained for the TM1-weak model with the additional hidden-strangeness meson fields introduced in a minimal fashion. Figure 2 shows the class of EoSs parametrized by $\Lambda_V$, the increase of $\Lambda_V$ produces a stiffer EoS. For comparison, the results for nonstrange matter for NL3 [12], TM1 [9] and

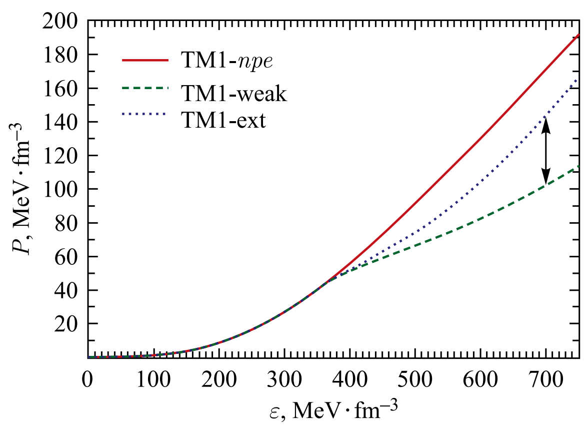


Fig. 1. The EoS calculated for the TM1 parameterization for nonstrange and strangeness-rich neutron star matter. The arrow indicates the additional stiffening of the EoS in the case of extended nonlinear model

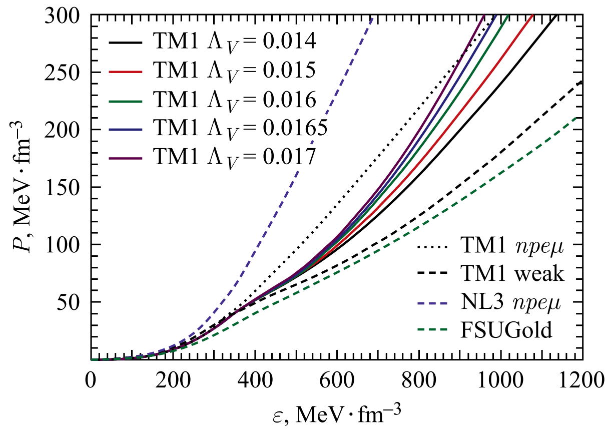


Fig. 2. The EoSs calculated for the extended nonlinear TM1 model for different values of $\Lambda_V$ form a distinct class with the stiffest EoS obtained for $\Lambda_V = 0.017$. Results obtained for selected models are included

FSUGold [13] parameterizations are included. Modification of the properties of neutron star matter concerns effective mass of baryons that arises from baryon interactions with the background nuclear matter. The numerical solutions predicted by Eq. (5) for the fixed value of the parameter $\Lambda_V = 0.0165$ both for the nonlinear model and for the TM1-weak model are shown in Fig. 3. The effective masses of strange baryons in the case of the nonlinear model drop less rapidly than the effective masses obtained in the TM1-weak model. Another interesting result is shown in Fig. 4, where the modification of vector meson masses is given.

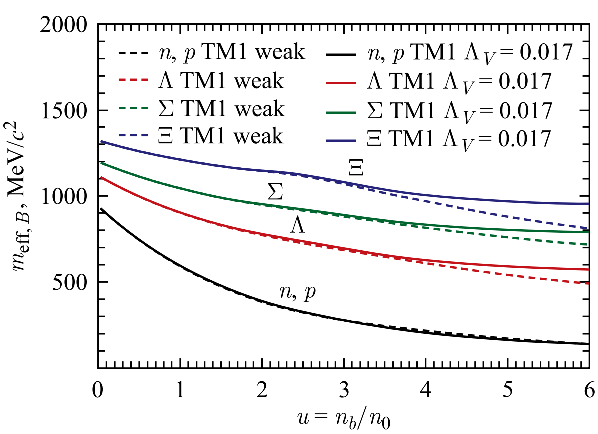


Fig. 3. The effective baryon masses

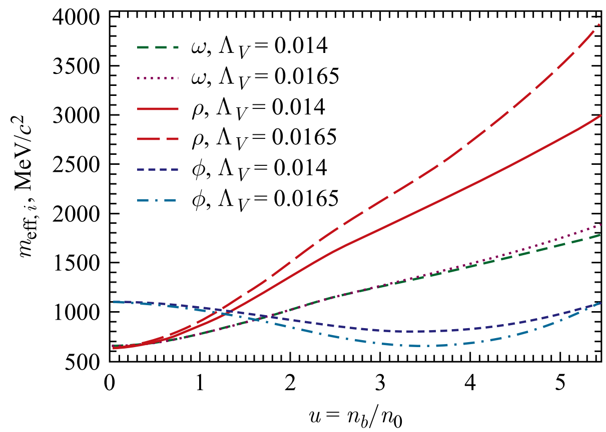


Fig. 4. The effective vector meson masses

The density dependence of the effective $\rho$ and $\phi$ vector meson masses led to the conclusion that their modification was produced by a strong $\Lambda_V$ dependence, especially in the high density limit. The effective mass of the $\omega$ meson is almost independent of the value of the parameter $\Lambda_V$. The stiffness of the EoS depends on the incompressibility of nuclear matter. In general, incompressibility comprises terms resulting from the kinetic pressure of Fermi gas and from the potential of the model. Factors that set an issue of the stiffness of the EoS are connected with differences between the strength of the effective repulsive and attractive forces. The strength of the effective repulsive force between strange baryons is mainly altered by the factor $1/m_{\mathrm{eff},\phi}$. The influence of the $\Lambda_V$ parameter on the density dependence of $1/m_{\mathrm{eff},\phi}$ is depicted in Fig. 5. The increase of the parameter $\Lambda_V$ considerably enhances the strength of the repulsive force in the system. A correct model of a neutron star requires the inclusion of additional EoSs that describe the matter of the inner and outer crusts. For the outer and inner crusts the EoSs of Baym, Pethick, and Sutherland (BPS) [14] and Baym, Bethe and Pethick (BBP) [15] have been used, respectively. The results obtained for the set of EoSs given in Fig. 2 led to the mass–radius relations. The mass–radius relations obtained for varying values of the parameter $\Lambda_V$ are shown in Fig. 6. The higher the value of $\Lambda_V$, the higher is the maximum mass of a

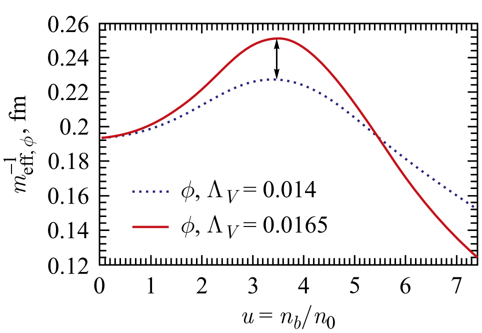


Fig. 5. The density dependence of the factor $1/m_{\mathrm{eff},\phi}$

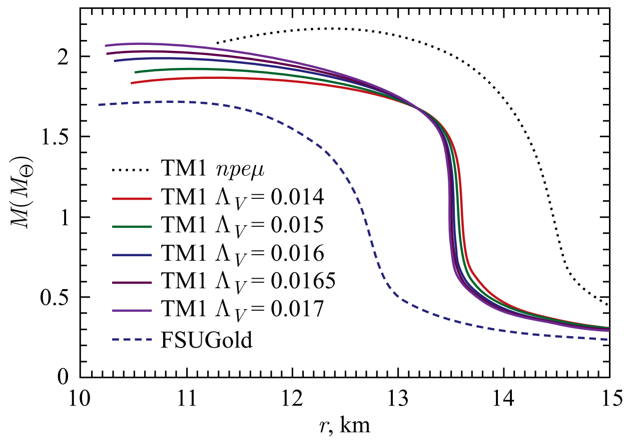


Fig. 6. The mass–radius relations

neutron star. The OTV equation offers the ability to characterize the properties of the interior of a neutron star. This can be done by finding solutions of the given equations for the radial distance from the center of the star. Thus, the composition and concentrations of hyperons in the inner part of a neutron star calculated in the nonlinear model can be traced for the chosen value of the parameter $\Lambda_V$. The radial dependence of the composition of the core of the maximum mass configuration is depicted in Figs. 8 and 9. The number density of $\Xi^-$ hyperons is reduced. However, an interesting feature of this model is the abundance of $\Sigma^-$ hyperons

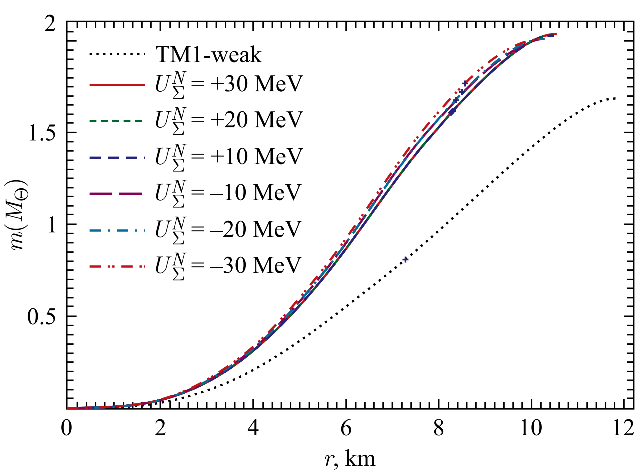


Fig. 7. Mass distributions for the maximum mass configurations

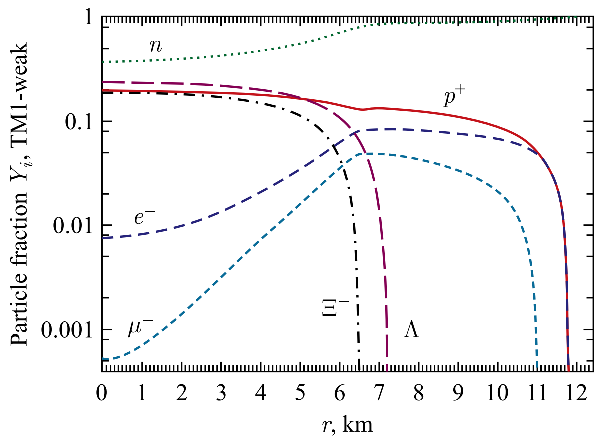


Fig. 8. The particle fraction $Y_i$ as a function of the radius of the neutron star, for the maximum mass configuration for the TM1-weak model with $\Lambda_V = 0.0165$

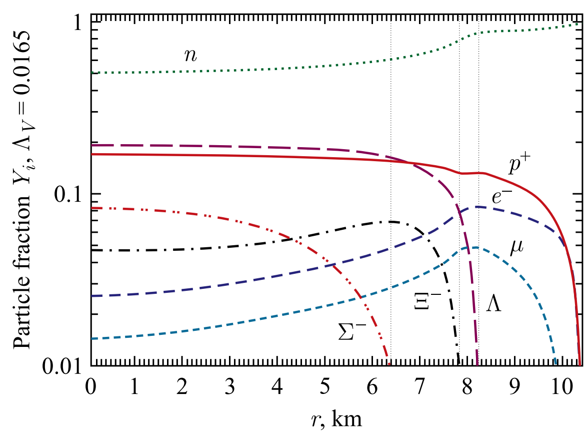


Fig. 9. The particle fraction $Y_i$ as a function of the radius of the neutron star, for the maximum mass configuration for the extended nonlinear model with $\Lambda_V = 0.0165$

in the core of the neutron star. There are still significant uncertainties associated with the experimental data on the hyperon–nucleus interactions. Thus, it is reasonable to investigate the effect of the hyperon–nucleus potential $U_Y^{(N)}$ on the obtained results [16]. Particular attention was paid to the dependence of the EoS on the $\Sigma$-nucleus potential $U_Y^{(\Sigma)}$. Detailed calculations were done for the selected values of the $U_\Sigma^{(N)}$ potential, assuming its both attractive and repulsive character. Calculations performed for the extended nonlinear model resulted in a sequence of EoSs. The stiffest one was obtained for the repulsive potential ($U_{\Sigma}^{(N)} = 30$ MeV). The influence of the $U_{\Sigma}^{(N)}$ potential on the internal structure of the maximum mass configuration is given in Fig. 7. This figure shows the distribution of mass in the interior of a neutron star for the extended model for different values of the $U_{\Sigma}^{(N)}$ potential and for the weak model. Dots indicate the boundary of the hyperon core.

## CONCLUSIONS

The characteristic feature of models that describe neutron star matter with nonzero strangeness is considerable softening of the EoS in comparison with the case when neutron star matter includes only nucleons. This softening of the EoSs leads to rather low values of the maximum neutron star masses achievable in theoretical models. This fact in turn is inconsistent with the observational results. In this paper the model with the more sophisticated sector of vector mesons was used to modify the high density limit of the EoS and to offer the possible solution of this problem. It was shown that the presence of different nonlinear vector meson couplings especially with the strange meson $\phi$ leads to the emergence of extra repulsive force in the strange sector of the system. Results of numerical calculations have shown that the nonlinear vector meson couplings significantly modify the in-medium properties of the effective baryon and meson masses. The nonlinear vector meson couplings modify both the asymmetry and strangeness content of the system and therefore lead to a model with a reduced strangeness and an enhanced asymmetry. The EoS for strangeness-rich matter of neutron stars calculated on the basis of the extended nonlinear model is much more stiffer than EoSs obtained for a neutron star with hyperons with the use of models in which vector meson $\phi$ is introduced in a minimal fashion (e.g., TM1-weak model). The consequences for the parameters of neutron stars are straightforward and appear as the considerable growth of neutron star masses.

### REFERENCES

1. *Chamel N., Haensel P.* Physics of Neutron Star Crusts // Living Rev. Relat. 2008. V. 11. P. 10.
2. *Bednarek I.* Hyperon Star // Acta Phys. Polon. B. 2009. V. 40. P. 3071.
3. *Demorest P. et al.* A Two-Solar-Mass Neutron Star Measured Using Shapiro Delay // Nature. 2010. V. 467. P. 1081.
4. *Antoniadis J. et al.* A Massive Pulsar in a Compact Relativistic Binary // Science. 2013. V. 340. P. 6131.

5. *Papazoglou P. et al.* Chiral Lagrangian for Strange Hadronic Matter // Phys. Rev. C: Nucl. Phys. 1998. V. 57. P. 2576.
6. *Papazoglou P. et al.* Nuclei in a Chiral $SU(3)$ Model // Phys. Rev. C: Nucl. Phys. 1999. V. 59. P. 411.
7. *Bednarek I., Manka R.* The Role of Nonlinear Vector Meson Interactions in Hyperon Stars // J. Phys. G: Nucl. Part. Phys. 2009. V. 36. P. 095201.
8. *Bednarek I. et al.* Hyperons in Neutron-Star Cores and a $2M_{\odot}$ Pulsar // Astron. Astrophys. 2012. V. 543. P. A157.
9. *Sugahara Y., Toki H.* Relativistic Mean Field Theory for Lambda Hypernuclei and Neutron Stars // Progr. Theor. Phys. 1994. V. 92. P. 803.
10. *Horowitz C. J., Piekarewicz J.* Neutron Star Structure and the Neutron Radius of $^{208}$Pb // Phys. Rev. Lett. 2004. V. 86. P. 5647.
11. *Schaffner J., Mishustin I. N.* Hyperon-Rich Matter in Neutron Stars // Phys. Rev. C: Nucl. Phys. 1995. V. 53. P. 1416.
12. *Lalazissis G. A. et al.* New Parametrization for the Lagrangian Density of Relativistic Mean Field Theory // Phys. Rev. C: Nucl. Phys. 1997. V. 55. P. 540.
13. *Todd-Rutel B., Piekarewicz J.* Neutron-Rich Nuclei and Neutron Stars: A New Accurately Calibrated Interaction for the Study of Neutron-Rich Matter // Phys. Rev. Lett. 2005. V. 95. P. 122501.
14. *Baym G. et al.* The Ground State of Matter at High Densities: Equation of State and Stellar Models // Astrophys. J. 1971. V. 170. P. 299.
15. *Baym G. et al.* Neutron Star Matter // Nucl. Phys. A. 1971. V. 175. P. 225.
16. *Weissenborn S. et al.* Hyperons and Massive Neutron Stars: The Role of Hyperon Potentials // Nucl. Phys. A. 2012. V. 881. P. 62.